Functionally specific optogenetic modulation in primate visual cortex

Mykyta M. Chernov[a,1], Robert M. Friedman[a], Gang Chen[b,c,d,e], Gene R. Stoner[f], and Anna Wang Roe[a,b,c,d,e,1]

[a]Division of Neuroscience, Oregon National Primate Research Center, Oregon Health & Science University, Beaverton, OR 97006; [b]Interdisciplinary Institute of Neuroscience and Technology, Qiushi Academy for Advanced Studies, Zhejiang University, Hangzhou 310029, China; [c]College of Biomedical Engineering and Instrument Science, Key Laboratory of Biomedical Engineering of Ministry of Education, Zhejiang University, Hangzhou 310027, China; [d]School of Medicine, Zhejiang University, Hangzhou 310058, China; [e]College of Biomedical Engineering and Instrument Science, Zhejiang Provincial Key Laboratory of Cardio-Cerebral Vascular Detection Technology and Medicinal Effectiveness Appraisal, Zhejiang University, Hangzhou 310027, China; and [f]Vision Center Laboratory, Salk Institute for Biological Studies, La Jolla, CA 92037

Edited by Tony Movshon, New York University, New York, NY, and approved August 17, 2018 (received for review February 6, 2018)

In primates, visual perception is mediated by brain circuits composed of submillimeter nodes linked together in specific networks that process different types of information, such as eye specificity and contour orientation. We hypothesized that optogenetic stimulation targeted to cortical nodes could selectively activate such cortical networks. We used viral transfection methods to confer light sensitivity to neurons in monkey primary visual cortex. Using intrinsic signal optical imaging and single-unit electrophysiology to assess effects of targeted optogenetic stimulation, we found that (*i*) optogenetic stimulation of single ocular dominance columns (eye-specific nodes) revealed preferential activation of nearby same-eye columns but not opposite-eye columns, and (*ii*) optogenetic stimulation of single orientation domains increased visual response of matching orientation domains and relatively suppressed nonmatching orientation selectivity. These findings demonstrate that optical stimulation of single nodes leads to modulation of functionally specific cortical networks related to underlying neural architecture.

primary visual cortex | functional connectivity | nonhuman primates | optogenetics | cortical columns

In primates, visual perception is mediated by brain circuits composed of nodes linked together in specific networks (1, 2). As revealed by anatomical tracing (3–10) and neuronal cross-correlation (11–14) studies, the anatomical substrates for processing of different features are mediated by connections between functionally specific cortical nodes (also termed columns, domains, and patches). In macaque monkey primary visual cortex (V1), ocular dominance (OD) columns (eye-specific nodes, ∼400 μm) tend to link to same-eye OD columns (3, 5), and orientation columns (orientation-specific nodes, ∼200 μm) tend to link to other columns of similar orientation preference (1–3, 6, 7). Given such functional specificity of intraareal connections, we hypothesized that stimulation of one node would preferentially activate other nodes in the same network. The capability to selectively activate such networks would introduce a functionally specific approach to neuromodulation of columnar networks and would be useful for the study of brain circuits, behavioral modulation, and potential treatment of disease.

Given the submillimeter size of these domains and their interconnections, appropriate tools are needed to visualize and modulate columnar activity. Previous attempts using electrical stimulation methods have been unable to selectively activate such functional networks, primarily due to electrical current spread. We hypothesized that light-based optogenetic (15–17) stimulation targeted to individual cortical nodes could selectively activate such cortical networks. We have previously shown that, through implanted optical windows, transfection of primate V1 and subsequent optical stimulation produce robust neuronal response, as assessed with electrophysiology and intrinsic signal optical imaging (18, 19).

In this study, we employed small-diameter (200-μm) fibers and fairly small vector injection volumes in primary visual cortex of anesthetized macaque monkeys. We predicted that optogenetic stimulation of a particular domain would modulate activity of related functional domains. That is, we predicted that stimulation of a single site would preferentially modulate (Fig. 1*A*) response of nearby same-eye columns (*Top Right*) and nearby orientation columns of similar orientation preference (*Bottom Right*). Alternatively, such optical stimulation could result in nonspecific activation that falls off with distance from the stimulation site (*Left*). Our results, based on intrinsic signal optical imaging, show that focal optogenetic stimulation can selectively affect networks that are eye-specific and orientation-selective.

Results

Optogenetic Stimulation Parameters. A total of 23 imaging sessions were conducted in three animals (monkeys A, B, and C; *SI Appendix*, Table S1). Our optogenetics procedures were similar to those in our previous studies except, to achieve more focal single-domain stimulation, we used single injections (vs. a cluster of injections), which resulted in a smaller transfection area (<1 vs. 4 mm^2; *SI Appendix*, Fig. S1), smaller optic fiber size (200 μm vs. 0.6 to 2 mm), and blue illumination to activate channelrhodopsin (ChR2) (vs. green illumination for C1V1, which gives greater tissue penetration) (*SI Appendix*, Table S2). The 200-μm-diameter optical fiber produced an effective stimulation diameter of ∼200 μm (Fig. 1*D*) and, given the previously published irradiance thresholds for ChR2 (16), produces focal light distribution (the effective illumination spot is equal to or less than the core diameter, as shown in

Significance

Primate visual cortex is organized into columns that process different features of a visual scene, such as color, orientation preference, and ocular dominance. Until now, their small size has made it difficult to modulate them directly. Here, we report for the first time that focal targeting of light-sensitive ion channels (channelrhodopsins) in macaques using lentiviral vectors allows one to stimulate functional domains. We show that such targeted stimulation leads to selective activation of anatomically connected neighboring domains with similar function. Such a fine-scale optical stimulation approach is capable of mapping functionally specific domain-based neuronal networks. Its potential for linking such networks to optogenetic modulation of perception and behavior opens doors for developing targeted, domain-based neuroprosthetics.

Author contributions: M.M.C., G.C., G.R.S., and A.W.R. designed research; M.M.C., R.M.F., and G.C. performed research; M.M.C., G.C., and A.W.R. analyzed data; and M.M.C., R.M.F., and A.W.R. wrote the paper.

The authors declare no conflict of interest.

This article is a PNAS Direct Submission.

[1]To whom correspondence may be addressed. Email: chernov@ohsu.edu or annawang@zju.edu.cn.

This article contains supporting information online at www.pnas.org/lookup/suppl/doi:10.1073/pnas.1802018115/-/DCSupplemental.

Published online September 26, 2018.

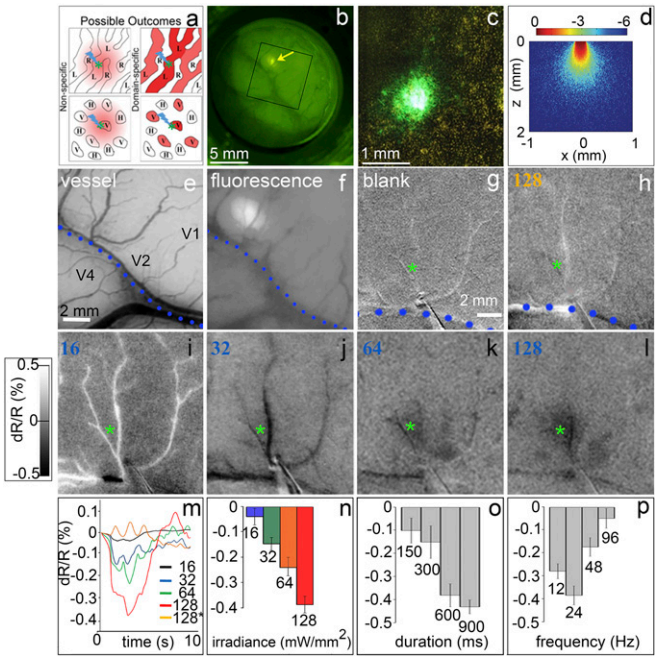

Fig. 1. Optogenetic stimulation induces intensity-dependent response. (*A*) Proposed model: Optogenetic stimulation of a functional domain (green star) leads to either nonspecific (*Left*) or domain-specific (*Right*) activation. Shown are OD columns (*Top*) and orientation domains (*Bottom*). (*B*) Four weeks after an injection of ChR2 viral vector in area V1. Arrow: viral expression ~1 mm in size. Fluorescence appeared about 3 wk postinjection, reached its maximum about 3 wk later, and persisted for the duration of the study (about 8 mo). The box refers to the field of view in *E* and *F*. (*C*) Fluorescence in the histological section of *B*. (*D*) Theoretical blue light distribution from a 200-μm core diameter fiber based on a Monte Carlo simulation (49). With the type of fiber used here, light falls off exponentially from the stimulation center such that the effective illumination spot (at least 5% of maximum illumination) is, at the irradiances used, equal to or less than the core diameter; this diameter is 200 μm in our case. Therefore, the light distribution is focal, and the effective diameter extends ~200 μm. (*E*) Blood vessel map. Dotted line: lunate sulcus. (*F*) Fluorescence of viral expression. Same image as the box in *B*. (Scale bar in *E* applies to *E*–*L*.) (*G*–*L*) Optical images from a single session of optogenetic stimulation (600 ms, 24 Hz, 20-ms pulse width) through a 200-μm optical fiber at different intensities. (*G*) No stimulation. (*H*) Orange, 593-nm, 128 mW/mm^2 stimulation. (*I*–*L*) Blue (473-nm) light stimulation, (*I*) 16, (*J*) 32, (*K*) 64, and (*L*) 128 mW/mm^2. Green asterisks: center of opsin expression and target of laser stimulation. Each image is the sum of 40 trials. (Intensity scale bar applies to *G*–*L*.) (*M*) Time courses of reflectance change in the area of expression. (*N*) Peak responses in *M*. (*O* and *P*) Peak responses to different stimulation durations at a frequency of 24 Hz and irradiance of 64 mW/mm^2 (*O*) and frequencies at a train duration of 600 ms and irradiance of 64 mW/mm^2 (*P*). Error bars are SE. Note: An increase in OI response magnitude is plotted as a negative reflectance change. All data are from monkey B.

Fig. 1*D*). This light distribution falls well within the extent of a single OD column (~400 μm) and is small enough to focus primarily on a single orientation column. Following transfection of the blue light-sensitive protein channelrhodopsin (ChR2-CaMKIIa-YFP, which expresses in excitatory neurons) in macaque V1 (Fig. 1 *A*–*C* and *SI Appendix*, Fig. S1), we targeted blue light (473 nm) to the expression site (Fig. 1 *E* and *F*) and examined whether the fluorescence truly indicated *ChR2-YFP* reporter gene expression.

Using intrinsic signal optical imaging (OI) to assess cortical response (note: negative reflectance change correlates with increased neuronal response), we found that focal optical stimulation produced robust OI reflectance change at the stimulated location and that this response increased with intensity (Fig. 1*G*, no stimulation; Fig. 1*I*, 16; Fig. 1*J*, 32; Fig. 1*K*, 64; and Fig. 1*L*, 128 mW/mm^2; quantified in Fig. 1*N*). Reflectance change time courses peaked within 2 to 3 s and peak magnitudes ranged from 0.05 to about 0.4%, typical of OI signals (Fig. 1 *M* and *N*). Control stimulation with orange (593-nm) light, away from the wavelength sensitivity of ChR2, failed to evoke a detectable response, even at a level eight times higher than the threshold irradiance for blue light (Fig. 1*H*). This confirmed that the cortical response is wavelength-specific and not due to thermal artifact. We further determined optimal stimulation parameters and found response magnitude leveled off at a duration of 600 ms (Fig. 1*O*) and peaked at 24 Hz (Fig. 1*P*). For subsequent experiments, we stimulated with 600-ms-long pulse trains at a frequency of 24 Hz. The irradiance varied between 16 and 128 mW/mm^2.

Ocular Dominance. We first examined whether focal stimulation would preferentially affect ocular dominance columns matching in eye preference. Stimulus conditions consisted of horizontal and vertical gratings presented to either the left eye or the right eye. As shown in Fig. 2*A*, using OI, we mapped OD columns in V1 (alternating left eye: light pixels; right eye: dark pixels) and examined the distribution of pixels activated by targeting an optical fiber to a single (right) eye column at the location of viral expression (green asterisk). Optogenetic stimulation at 16 mW/mm^2 produced a focal site of activation (Fig. 2*B*). Almost all (over 95%) of the significantly activated pixels (blue, significant activation over blank; two-tailed *t* test, $P < 0.05$) fell into the right-eye columns. Increasing the stimulation intensity (64 mW/mm^2) increased the area of activation; however, most pixels (>95%) within this larger area remained confined to the same- (right-) eye columns (Fig. 2*C*). A second example from V1 of another animal is shown in Fig. 2 *D*–*F* (images are shown in *SI Appendix*, Fig. S2). Again, optogenetic activation is almost exclusively confined to OD columns of the stimulated eye column (Fig. 2*E*), even when stimulation intensity leads to greater activation (Fig. 2*F*). The extent of columnar activation spans roughly three OD columns of the same eye, consistent with anatomical studies of intercolumnar connectivity (3, 5). To further test whether these effects could be due simply to distance, we conducted a two-factor linear regression by sampling a region of cortex around the stimulation site (250-μm regions of interest; spacing 500 μm; *SI Appendix*, Fig. S3). This analysis demonstrated that OD is the better predictor of change in OI signal magnitude than distance. These data support the hypothesis that targeted optogenetic stimulation activates eye-specific intracortical connectivity.

We next examined whether adding optogenetic stimulation (opto) to ongoing visual stimulation would have functionally specific effects. To address this, runs consisted of 10 randomly

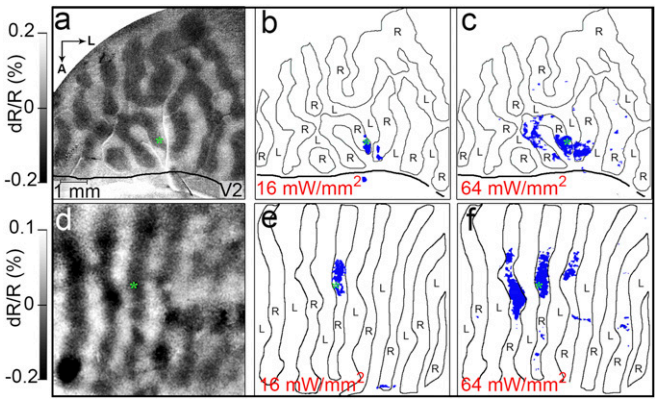

Fig. 2. Optogenetic stimulation of single eye column has eye-specific effects. (*A*) OD map (monkey B, same site as in Fig. 1 studied in a separate session): right- (R) vs. left- (L) eye subtraction map, outlined in *B* and *C*. (*B* and *C*) Optical stimulation with intensities at (*B*) 16 mW/mm^2 and (*C*) 64 mW/mm^2 (600 ms, 24 Hz, 20-ms pulse width). Green asterisks: center of opsin expression and target of laser stimulation. Optical stimulation in right-eye column leads to focal activation confined to same-eye column (blue pixels: significant activation over blank, $P < 0.05$). Thick solid lines mark the V1/V2 border. (*D*–*F*) Similar results from monkey C (see also *SI Appendix*, Fig. S2). (Scale bar in *A* applies throughout the figure.) A, anterior; L, lateral.

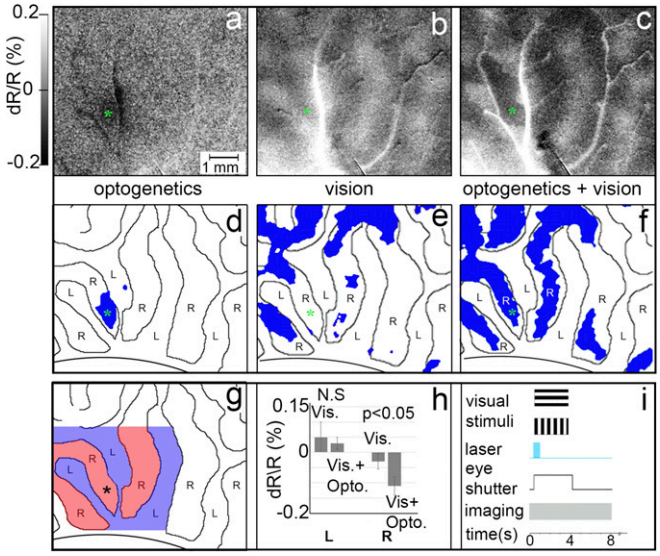

Fig. 3. Optogenetic stimulation enhances eye-specific visual response. (*A–C*) Optical images in response to *A* optogenetic stimulation alone (32 mW/mm^2 versus blank), (*B*) presentation of visual stimuli alone (left eye minus right eye), and (*C*) presentation of visual stimuli combined with optogenetic stimulation (left eye + laser versus right eye + laser). (Intensity scale bar applies to *A–C*.) From monkey B. (*D–F*) Significantly activated pixels (blue; $P < 0.05$) in *A–C*, with left-eye and right-eye OD columns outlined. (*G* and *H*) Quantification of peak reflectance change of all significant pixels near the optogenetic stimulation site (up to 3 OD columns away). (*G*) Colored region: area quantified. Blue, left-eye OD columns; red, right-eye OD columns. Asterisk: center of viral expression site and target of laser stimulation. (*H*) Reflectance change magnitude for same-eye (right-eye) and opposite-eye (left-eye) columns. Error bars are SD. For the opposite- (L) eye OD columns, there is no significant difference between vision alone vs. blank and vision+optogenetic stimulation vs. blank conditions. For the same (R) eye, optogenetic stimulation significantly enhances the response (*t* test, $P < 0.05$). Note: An increase in OI response magnitude is plotted as a negative reflectance change. (Scale bar in *A* applies to *A–G*.) (*I*) Timing of visual presentation, optogenetic laser stimulation, optical imaging, and control of eye shutters. N.S., not significant.

interleaved conditions: two orientations × two eyes × opto/no opto, an opto-alone condition, and a blank condition. OD and orientation maps were generated from visual conditions, and OD-opto and orientation-opto from visual+opto conditions. We compared optogenetic stimulation alone, visual presentation alone, and the visual+opto condition (Fig. 3 *A–C*; stimulation and image acquisition timing are shown in Fig. 3*I*). As above, optogenetic stimulation alone (32 mW/mm^2) resulted in fairly focal activation confined to the stimulated (right-eye) OD column (Fig. 3*A*; blue pixels in Fig. 3*D*, significantly activated over blank). Fig. 3*B* shows the OD map obtained in response to visual stimulation alone (blue pixels in Fig. 3*E*, preference for right eye over left eye). We found that addition of optogenetic stimulation to ongoing visual stimulation results in a focal enhancement of same-eye OD columns. As seen in Fig. 3*F*, combined visual stimulus presentation (right- or left-eye visual stimulation) and optogenetic stimulation (laser in right-eye column) results in a greater number of significantly activated pixels in the right-eye OD column than with visual stimulus presentation alone. This is quantified in Fig. 3*H*, which shows that these pixels fall within the same-eye (Fig. 3*H*, *Right*) but not the opposite-eye columns (Fig. 3*H*, *Left*; no significant difference between vision+laser and vision alone). This enhancement effect was observed up to about two OD columns away from the laser stimulation site. Stimulation at sites distant from the viral expression site did not show such effects. Thus, optogenetic enhancement of visual response appears to be confined to the OD columns associated with the stimulated eye column, consistent with mediation via eye-specific intraareal connectivity.

Orientation. Orientation networks are another functionally specific network within V1. As demonstrated via anatomical tracer studies as well as physiological spike train cross-correlation studies, orientation domains within V1 are preferentially connected with other domains of similar orientation preference (1–3, 6, 7). We therefore predicted that, if the optogenetic stimulation is mediated via these intracortical connections, one should observe orientation-specific effects of such stimulation. After confirming that our orientation domain imaging maps were reproducible and stable (*SI Appendix*, Fig. S4), we targeted single orientation domains and compared orientation maps obtained without and with such focal stimulation. Fig. 4*A* illustrates an orientation OI map (red pixels: significant preference for horizontal gratings; blue pixels: significant preference for vertical gratings; two-tailed *t* test, $P < 0.05$). After targeting a vertical domain in the center of the transfected site for optogenetic stimulation (green asterisk), we compared orientation subtraction maps obtained with optogenetic stimulation with those without optogenetic stimulation. We predicted enhancement of matched orientation response (as measured in both increased magnitude of domain response and an increase in the number of pixels that reach significance). Since previous studies have shown that local anatomical connections span roughly 2 to 3 mm, we expected the strongest effects within this region of influence.

We analyzed the number of pixels preferring vertical (blue) vs. horizontal (red) within a 2-mm radius of the stimulation site (dashed yellow circles in Fig. 4) without (Fig. 4*A*) and with (Fig. 4*B*) optogenetic stimulation. As predicted, when a single vertical orientation domain was optogenetically stimulated, the total area of vertically preferring response increased (the number of significant pixels shifted toward vertical, blue, and away from horizontal, red; Fig. 4*C*; $\chi^2 = 18.29$, $P < 0.001$). A second case, shown in Fig. 4 *G* and *H* (precise fiber location targeting a blue domain shown in *SI Appendix*, Fig. S5*B*), demonstrates a similar shift in the number of vertical to horizontal pixels with stimulation (Fig. 4*I*; $\chi^2 = 10.31$, $P = 0.001$). We also examined the effect of stimulation domain by domain. We observed that the domain locations in the unstimulated and stimulated maps were stable (*SI Appendix*, Fig. S5*B*); for a few domains, if stimulation effect was large, a domain would "emerge" or "disappear" (relative to the *t*-statistic threshold). We saw either an increase in pixel number for matching orientation domains or a decrease for nonmatching orientation domains (Fig. 4*D*: vertical, nine domains; horizontal, four domains; Fig. 4*J*: vertical, 17 domains; horizontal, 12 domains; see analysis in *SI Appendix*, Fig. S5*B*). When examined domain by domain (Fig. 4 *E* and *K*), a greater number of pixels achieved significance in vertical domains and fewer pixels did in horizontal domains (Wilcoxon signed-rank test; Fig. 4*E*, not significant due to the small number of domains; Fig. 4*K*, $P < 0.05$). In addition, optogenetic stimulation increased the signal magnitude of vertical domains (Fig. 4 *F* and *L*; $P < 0.05$). In the horizontal-preferring domains, there was significant decrease in one case (Fig. 4*L*; $P < 0.05$) and no significant change in the other (Fig. 4*F*; $P = 0.09$). Finally, if the analysis was extended beyond a radius of 2 mm to include the entire field of view, for both cases we found that the differences between stimulated and unstimulated conditions no longer become statistically significant ($P > 0.05$). This suggests that the inclusion of domains outside the 2-mm radius dilutes the difference seen for connected domains and further supports the finding that optogenetic stimulation has a focal effect which diminishes with distance, which we found to be a statistically significant factor (*SI Appendix*, Fig. S3). These measures confirm a relative enhancement of domains matching in preference to the optically stimulated domain and a relative (weaker) suppression of orthogonal domains.

Neuronal Response. To assess whether neuronal spike firing underlies the optical imaging results, we performed a series of electrophysiological recordings in two animals. We found that, in comparison with our previous studies in awake monkeys, the hit rate of optogenetically activated neurons in this study was much lower (12 units in nine penetrations at the site of viral transfection); this was expected given the effects of anesthesia,

NEUROSCIENCE

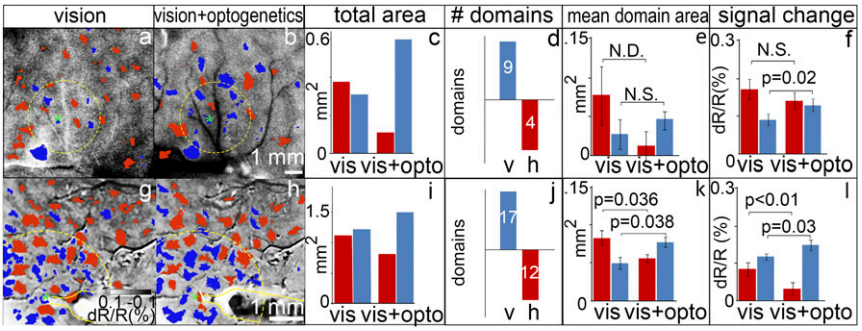

Fig. 4. Optogenetic stimulation enhances visual responses in matched orientation domains. (*A* and *B*) Orientation subtraction maps (horizontal minus vertical) in the absence (*A*) and presence (*B*) of optogenetic stimulation (600 ms, 24 Hz, 64 mW/mm^2) of a vertical domain (asterisks: center of opsin expression site and target of laser stimulation). Red pixels: significant horizontal activation; blue pixels: significant vertical activation (two-tailed *t* test). Same site of stimulation as in Fig. 3*A* from monkey B. (*C*) Quantification of red and blue pixels around (2-mm radius, indicated by yellow dotted circles) the transfection site in *A* and *B* shows optogenetic stimulation produces a shift toward greater vertical domain response ($\chi^2 = 18.29$, $P < 0.001$). (*D*) Number of domains (vertical, V, blue; horizontal, h, red) that increase (upward bar graphs) or decrease (downward bar graphs) in area. (*E*) Average area of each domain in mm^2 (Wilcoxon signed-rank test; not significant due to the small number of domains). Error bars are SE. (*F*) Magnitude of the response from each domain (d*R*/*R*) (Wilcoxon signed-rank test, $P < 0.05$). Error bars are SE. (*G*–*L*) Similar results from monkey C. Yellow outlines in *G* and *H* indicate optical fiber position, targeting the blue domain. (Intensity scale bar in *G* applies to *A*, *B*, *G*, and *H*. Scale bar in *B* applies to *A* and *B*; scale bar in *G* applies to *G* and *H*.) N.S., not significant.; N.D., not enough data for statistical test. See images enlarged in *SI Appendix*, Fig. S5*A*.

smaller transfection area, and smaller optic fiber size (*SI Appendix*, Table S2). Despite this, optogenetic modulation of visually responsive neurons was readily observed. We evaluated whether these effects were related to ocular dominance.

We predicted that there would be distinct effects on same-eye and opposite-eye columns. Fig. 5*A* shows the findings from 26 penetration sites from one animal. Although the population sample is small, it is an extensive, dense sampling from a small region of cortex, not often seen in optical imaging experiments. The sites are shown in relation to the OD map and are centered in and around the viral vector injection site (centered in a left-eye column; yellow circle). While none of these neurons responded to optogenetic stimulation alone, we observed diverse types of effects when optogenetic stimulation was added to visual stimulation. Fig. 5*B* illustrates examples of neurons in which visual response was enhanced by optogenetic stimulation (red), decreased (blue), and not significantly changed (green) (*Left*, vision alone; *Right*, vision+optogenetic stimulation). In the population of 26 neurons (Fig. 5*C*), 9 exhibited enhancement (red), 5 exhibited relative suppression (blue), and 12 were not significantly changed (green). Note that responses to visual and optogenetic stimulation are comparable in magnitude, indicating optogenetic stimulation induces a response within a normal physiological range (19).

We further examined the relationship of these responses to the ocular dominance map. As shown in Fig. 5*D*, by examining units in the same- and opposite-eye OD columns, almost all (seven of the nine; red) of the neurons that show enhanced responses lie within the same OD column as the optogenetic stimulation site, while four of the five neurons (blue) with suppressed response lie in the opposite-eye column ($\chi^2 = 4.38$, $P = 0.036$). Those that were not significantly modulated (green) were found in both eye columns ($n = 6$ in each of the same- and opposite-eye columns). Thus, consistent with our predictions, there were distinct effects on same- vs. opposite-eye columns. These findings were corroborated by results of a generalized linear model with OD column location and distance away from the center of stimulation as independent variables and change in firing rate as the dependent variable. OD column location was found to be statistically significant ($P < 0.05$) while distance from the center was not ($P = 0.3$). However, the interaction between OD column and distance was statistically significant ($P < 0.05$), suggesting that far-away OD columns may be activated less than those closer to the stimulation site.

These observed neuronal responses are, as a population, consistent with the eye-specific effects observed with optical imaging. In sum, while optogenetic stimulation can modulate the neuronal firing rate of cells responding to visual stimuli, this modulation appears excitatory between same-eye OD columns and tends toward inhibitory between opposite OD columns. These results agree with known functional relationships between eye-specific columns in V1.

We have presented the OD and orientation effects independently. However, we would like to make clear that both effects occur simultaneously. In some cases, when the intensity is just right, we do observe both effects. That is, with optogenetic stimulation alone, in some cases we observe fluctuation of intensity within OD activations that is consistent with the spacing of orientation domains (*SI Appendix*, Fig. S6).

Discussion

We have shown, using optical imaging methods, that targeted and focal optogenetic stimulation enhances neighboring same-eye OD columns (Figs. 2 and 3). In addition, stimulation of an orientation column can enhance the response of nearby like-oriented domains and relatively suppresses those of orthogonal selectivity (Fig. 4). Recorded neuronal ocular dominance responses are consistent with these imaging results (Fig. 5). While these OD and orientation results were presented separately, they are co-occurring effects (*SI Appendix*, Fig. S6). This finding is in contrast to that in the tree shrew, where optogenetic and visual stimuli summed in a spatially isotropic fashion, suggesting a difference either in stimulation methodology or in functional connectivity across species (20).

We suggest that the OD column- and orientation-specific effects may be mediated, at least in part, by intrinsic horizontal connections in macaque V1. Anatomically, there exists a prevalence of connectivity between same-eye columns over opposite-eye columns (3, 5). Horizontal connections are patchy and link columns of similar functional preference such as color (1, 2, 12) and orientation (1, 2, 6, 7, 11). As shown by studies using optical imaging and electrophysiology, these local connections mediate synaptic interactions (both facilitatory and suppressive) between orientation-matched columns but not between orthogonal orientation domains, and serve to change the balance of excitatory and suppressive surround effects (21–24). Consistent with these studies, addition of optogenetic stimulation to ongoing activity biases the network toward the preference of the stimulated column and away from the orthogonal network. We also note that the extent of these direct horizontal networks in V1 span roughly 2 to 3 mm (3, 5), similar to the extent of effects on ocular dominance activation shown in Fig. 2. While feedforward and feedback effects may also be evoked by optogenetic stimulation, these effects are weaker in the anesthetized animal. Thus, the optogenetic effects are consistent with previously observed functional selectivity (excitatory/matched and suppressive/nonmatched) and spatial extent of horizontal connectivity in V1. While the anatomical specificity of these intracortical connections

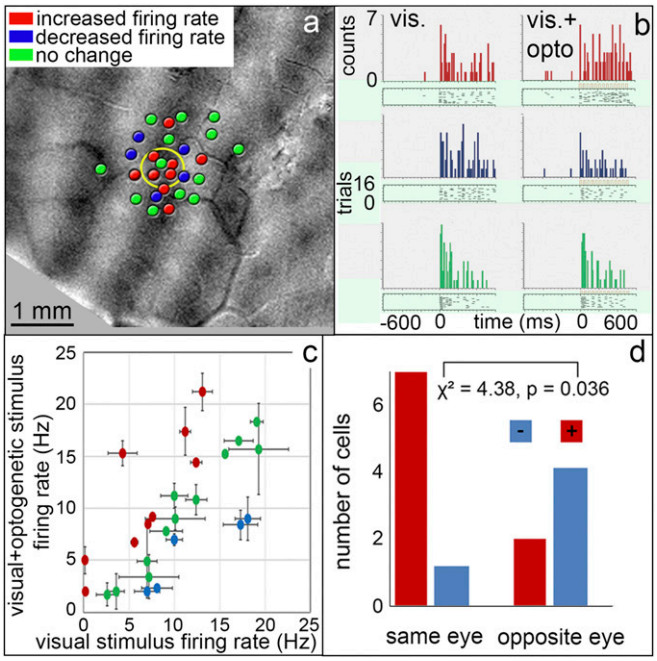

Fig. 5. Single-neuron responses are modulated in an eye-specific manner by optogenetic stimulation. (*A*) Twenty-six electrode penetrations at or near the optogenetic injection site (yellow circle), shown on an OD map (dark, right eye; light, left eye). None of these neurons responded to optogenetic stimulation alone. From monkey C. (*B*) Poststimulus time histograms and raster plots of three example units in response to presentation of preferred grating [*Left* (within the brackets)] and when visual stimulation was combined with optogenetic stimulation [*Right* (within the brackets)]; irradiance: 128 mW/mm^2; duration: 600 ms; frequency: 24 Hz; average 16 trials. Responses exhibit significant increase (red), decrease (blue), and no significant change (green) in number of spikes (paired *t* test, $P < 0.05$). (*C*) Of the 26 units recorded, 9 exhibited a significant increase (red), 5 a decrease (blue), and 12 no change (green) in firing rate with optogenetic stimulation. Error bars are SD. (*D*) Eye-specific effect. Red units, those enhanced by optogenetic stimulation, tended to fall within the same-eye OD column (7 of 9); blue units, those decreased by optogenetic stimulation, tended to fall in the opposite-eye column (4 of 6) ($\chi^2 = 4.38$, $P < 0.05$). Green units were found in both eye columns.

has been known, this study demonstrates optogenetically mediated modulation of such specific circuits in macaque visual cortex in vivo.

We relate these circuit modulations to previous studies of binocular integration in V1. It is known that, while binocular presentation can enhance the response of binocular neurons over monocular presentation, this facilitation happens only if the stimulations in the two eyes are appropriately matched. Parameters which contribute to match dependence include orientation, contrast, and phase (e.g., refs. 25–29). For example, response of binocular neurons in V1 of cats and monkeys is enhanced by orientation-matched stimulation of the other eye and relatively suppressed by orthogonal stimulation of the other eye (30–32). Such a finding is consistent with our findings of orientation-matched enhancement and nonmatched suppression following optogenetic stimulation of single orientation domains. We suggest potential applications of this method for further study of stereopsis (33, 34), binocular rivalry (35), and strabismus and amblyopia (36).

There are a growing number of studies using optogenetic stimulation for studying cortical circuitry and behavior in nonhuman primates (17–19, 37–44). We show that targeted optogenetic stimulation offers the ability to selectively stimulate single cortical columns to probe cortical circuits in nonhuman primates. Historically, using electrical stimulation, it has been difficult to selectively stimulate specific functional domains due to (*i*) their small size, (*ii*) current spread accompanying electrical stimulation, (*iii*) the presence of both orthodromic and antidromic activation, and (*iv*) effects on fibers of passage (45). Viral transfection with opsins, on the other hand, allows for relatively sparse and focal labeling of cells within a small region. It also allows one to pick a subset of neuronal types by choosing an appropriate promoter for opsin expression (42, 46). Stimulation can therefore be confined to a specific functional domain and can minimize undesired activation of neighboring functionally distinct neuronal populations. It is important to recognize that the same neuron is part of multiple networks. Using relevant visual stimuli and image subtractions reveals the effect of focal stimulation on particular functional networks. Thus, our results demonstrate the power of optogenetic stimulation to selectively bias anatomical network activations underlying ongoing activity in primates. This enabled us to show the extent to which underlying architecture constrains the effects of optogenetic stimulation and the importance of using appropriate stimulation criteria for addressing questions of cortical circuitry. The feasibility of achieving functionally selective cortical modulation via focal, targeted optogenetic neuromodulation opens new vistas for studying cortical circuitry and for developing targeted cortical prosthetics in human and nonhuman primates.

Methods

Subjects. All procedures were carried out with prior approval of the Vanderbilt University Institutional Animal Care and Use Committee and in accordance with NIH animal welfare guidelines. In three adult macaques, we conducted the study of different optical irradiance levels in one animal and optical imaging and electrophysiology in the other two, for a total of 23 experimental sessions (*SI Appendix*, Table S1). After the conclusion of the experiments, the animals were deeply anesthetized and euthanized.

Viral Vector Injections. The surgical procedures used for implantation of chronic optical chambers and viral vector injections have been described elsewhere (18, 19). Briefly, we injected, under isoflurane anesthesia using a picospritzer, a lentiviral vector with a deficient HIV viral envelope pseudotyped with a vesicular stomatitis virus glycoprotein and carrying a modified channelrhodopsin [ChR2(H134R)] linked to a CaMKIIa promoter and enhanced yellow fluorescent protein reporter gene (University of Pennsylvania).

Optical Imaging. For details on the optical imaging methods, see refs. 18 and 47. Following expression (typically 4 to 6 wk), a chronic optical window was implanted over the expression site and a series of optical imaging and electrophysiology experiments were conducted under anesthesia, either brevital (1 mg·kg^{-1}·h^{-1}), or propofol (18 mg·kg^{-1}·h^{-1}) and ketamine (2.5 mg·kg^{-1}·h^{-1}), supplemented with up to 1% isoflurane in oxygen. To prevent eye movements, animals were paralyzed with i.v. rocuronium bromide (1 mg·kg^{-1}·h^{-1}). OI imaging was performed under 632-nm illumination, at 4 frames per s, with a minimum of 8-s interstimulus interval (ISI). An Optical Imaging Inc 3001 VDAQ system was used to collect intrinsic signals.

Visual Stimuli. High-contrast square-wave gratings (horizontal or vertical, 1° per cycle, 4 cycles per s) were presented to each eye through the use of electromechanical shutters. Blocks of stimulus conditions were presented in a randomly interleaved fashion. These consisted of visual stimulation alone (four conditions: left eye horizontal, left eye vertical, right eye horizontal, right eye vertical) and visual+laser stimulation conditions (four conditions: each visual stimulus condition presented together with optogenetic stimulation). Blank condition: eye shutters closed, no laser stimulation. ISI: gray screen (luminance: mean of the grating stimuli). From these single-condition maps, two OD and two orientation maps were generated: OD [all right (R) minus all left (L)], OD+opto [all (R+opto) minus all (L+opto)], orientation [all horizontal (H) minus all vertical (V)], and orientation+opto [all (H+opto) minus all (V+opto)]. Thus, a typical block consisted of four visual-only conditions, four visual+opto conditions, one optogenetic stimulation-alone condition, and one blank condition, for a total of 10 conditions. Conditions within each block of trials were randomized (>30 trials per condition). Timing is shown in Fig. 3*I*. In assessment of optogenetic stimulation-alone parameters (Fig. 1), laser stimulation conditions varied in either irradiance, duration, or frequency.

Optogenetic Stimulation. We delivered optical stimulation through an optical chamber (18). We determined optimal frequency (range 12 to 96 Hz), duration (150 to 900 ms), and optical power (16 to 128 mW/mm^2). Pulse width was 20 ms. Optogenetic stimulation was performed using a 473-nm (blue) diode laser (Shanghai Laser), with a 593-nm (orange) diode laser (Shanghai

Laser) serving as a control. Both light sources were coupled to the same 200-μm-diameter silica core multimode optical fiber (N.A. 0.44) using a series of dichroic mirrors and a reflective collimator.

Electrophysiology. Single-unit recordings were acquired using tungsten microelectrodes (impedance 1 to 2 MΩ) connected to an A-M Systems headstage and amplifier. A Blackrock Microsystems Data Acquisition System (Cerebus) was used for spike sorting and detection and analog-to-digital conversion at 30 kHz. Visual stimuli were the same as described above (moving gratings), presented to both eyes. Both vertical and horizontal gratings were initially presented to each cell, and the stronger stimulus of the two was chosen for data acquisition and analysis.

Data Analysis. Optical intrinsic signal (OIS) data frames were analyzed using custom MATLAB scripts written by members of the lab (MathWorks). To examine signal change from baseline, the first frame of each condition was subtracted from the rest of the image sequence. Conditions from all trials (>30 per condition) were averaged to increase signal-to-noise ratio. To remove large reflectance changes due to vascular artifact, pixels with absolute values greater than 1 SD from the median were excluded. Images were filtered with a Gaussian low-pass filter (5-pixel, 0.1-mm kernel) and a median high-pass filter (2-mm kernel). In each session, OD and orientation maps were obtained from the same images but summed differently. OD maps were obtained by subtracting sums of left-eye and of right-eye conditions and then outlined using magic wand in Adobe Photoshop (luminance tolerance of 32). Orientation maps were obtained by subtracting the maps of horizontal and vertical gratings. Pixels with statistically significant reflectance changes were determined using a two-tailed t test (with Bonferroni correction, $P < 0.05$). Electrophysiological data were spike-sorted manually using a hoop algorithm (48). For each unit, each recording contained at least 40 trials, and custom MATLAB scripts were used to construct raster plots and perievent stimulus histograms. Significant change in firing rate was assessed with paired t test. To test whether changes in firing rate following combined optogenetic and visual stimulus presentation were functional domain-dependent, we constructed a generalized linear model with OD column location and distance away from the center of stimulation as independent variables and change in firing rate as the dependent variable.

Histology. Following euthanasia [Beuthanasia (Merck Animal Health); 0.25 mL/kg, i.v.], the animals were perfused with 4% paraformaldehyde. Brains were removed, and tissue was sliced at 40 μm and imaged with a fluorescence microscope.

ACKNOWLEDGMENTS. This research was conducted at Zhejiang University, Oregon Health & Science University, and Vanderbilt University, and was supported by National Natural Science Foundation Grants 81430010, 31627802 (to A.W.R.), and 31471052 (to G.C.); National Hi-Tech Research and Development Program Grant 2015AA020515 (to A.W.R.); Zhejiang Provincial Natural Science Foundation of China Grant LR15C090001 (to G.C.); Fundamental Research Funds for the Central Universities Grant 2015QN81007 (to G.C.); NIH EY022853 (to G.R.S. and A.W.R.); Oregon Health & Science University Institutional funds (to A.W.R.); the Vanderbilt Vision Research Center; and Center for Integrative and Cognitive Neuroscience at Vanderbilt.

1. Livingstone MS, Hubel DH (1984) Anatomy and physiology of a color system in the primate visual cortex. *J Neurosci* 4:309–356.
2. Livingstone MS, Hubel DH (1984) Specificity of intrinsic connections in primate primary visual cortex. *J Neurosci* 4:2830–2835.
3. Malach R, Amir Y, Harel M, Grinvald A (1993) Relationship between intrinsic connections and functional architecture revealed by optical imaging and in vivo targeted biocytin injections in primate striate cortex. *Proc Natl Acad Sci USA* 90:10469–10473.
4. Amir Y, Harel M, Malach R (1993) Cortical hierarchy reflected in the organization of intrinsic connections in macaque monkey visual cortex. *J Comp Neurol* 334:19–46.
5. Yoshioka T, Blasdel GG, Levitt JB, Lund JS (1996) Relation between patterns of intrinsic lateral connectivity, ocular dominance, and cytochrome oxidase-reactive regions in macaque monkey striate cortex. *Cereb Cortex* 6:297–310.
6. Bosking WH, Zhang Y, Schofield B, Fitzpatrick D (1997) Orientation selectivity and the arrangement of horizontal connections in tree shrew striate cortex. *J Neurosci* 17:2112–2127.
7. Sincich LC, Blasdel GG (2001) Oriented axon projections in primary visual cortex of the monkey. *J Neurosci* 21:4416–4426.
8. Sincich LC, Horton JC (2002) Divided by cytochrome oxidase: A map of the projections from V1 to V2 in macaques. *Science* 295:1734–1737.
9. Federer F, et al. (2009) Four projection streams from primate V1 to the cytochrome oxidase stripes of V2. *J Neurosci* 29:15455–15471.
10. Yarch J, Federer F, Angelucci A (2017) Local circuits of V1 layer 4B neurons projecting to V2 thick stripes define distinct cell classes and avoid cytochrome oxidase blobs. *J Neurosci* 37:422–436.
11. Ts'o DY, Gilbert CD, Wiesel TN (1986) Relationships between horizontal interactions and functional architecture in cat striate cortex as revealed by cross-correlation analysis. *J Neurosci* 6:1160–1170.
12. Ts'o DY, Gilbert CD (1988) The organization of chromatic and spatial interactions in the primate striate cortex. *J Neurosci* 8:1712–1727.
13. Roe AW, Ts'o DY (1999) Specificity of color connectivity between primate V1 and V2. *J Neurophysiol* 82:2719–2730.
14. Roe AW, Ts'o DY (2015) Specificity of V1-V2 orientation networks in the primate visual cortex. *Cortex* 72:168–178.
15. Fenno L, Yizhar O, Deisseroth K (2011) The development and application of optogenetics. *Annu Rev Neurosci* 34:389–412.
16. Boyden ES, Zhang F, Bamberg E, Nagel G, Deisseroth K (2005) Millisecond-timescale, genetically targeted optical control of neural activity. *Nat Neurosci* 8:1263–1268.
17. Diester I, et al. (2011) An optogenetic toolbox designed for primates. *Nat Neurosci* 14: 387–397.
18. Ruiz O, et al. (2013) Optogenetics through windows on the brain in the nonhuman primate. *J Neurophysiol* 110:1455–1467.
19. Nassi JJ, Avery MC, Cetin AH, Roe AW, Reynolds JH (2015) Optogenetic activation of normalization in alert macaque visual cortex. *Neuron* 86:1504–1517.
20. Huang X, Elyada YM, Bosking WH, Walker T, Fitzpatrick D (2014) Optogenetic assessment of horizontal interactions in primary visual cortex. *J Neurosci* 34:4976–4990.
21. Weliky M, Kandler K, Fitzpatrick D, Katz LC (1995) Patterns of excitation and inhibition evoked by horizontal connections in visual cortex share a common relationship to orientation columns. *Neuron* 15:541–552.
22. Sato H, Katsuyama N, Tamura H, Hata Y, Tsumoto T (1996) Mechanisms underlying orientation selectivity of neurons in the primary visual cortex of the macaque. *J Physiol* 494:757–771.
23. Toth LJ, Rao SC, Kim DS, Somers D, Sur M (1996) Subthreshold facilitation and suppression in primary visual cortex revealed by intrinsic signal imaging. *Proc Natl Acad Sci USA* 93:9869–9874.
24. Dragoi V, Sharma J, Sur M (2000) Adaptation-induced plasticity of orientation tuning in adult visual cortex. *Neuron* 28:287–298.
25. Sengpiel F, Blakemore C (1994) Interocular control of neuronal responsiveness in cat visual cortex. *Nature* 368:847–850.
26. Sengpiel F, Blakemore C, Harrad R (1995) Interocular suppression in the primary visual cortex: A possible neural basis of binocular rivalry. *Vision Res* 35:179–195.
27. Cavanaugh JR, Bair W, Movshon JA (2002) Selectivity and spatial distribution of signals from the receptive field surround in macaque V1 neurons. *J Neurophysiol* 88:2547–2556.
28. Xu WF, Shen ZM, Li CY (2005) Spatial phase sensitivity of V1 neurons in alert monkey. *Cereb Cortex* 15:1697–1702.
29. Song XM, Li CY (2008) Contrast-dependent and contrast-independent spatial summation of primary visual cortical neurons of the cat. *Cereb Cortex* 18:331–336.
30. Barlow HB, Blakemore C, Pettigrew JD (1967) The neural mechanism of binocular depth discrimination. *J Physiol* 193:327–342.
31. Poggio GF, Fischer B (1977) Binocular interaction and depth sensitivity in striate and prestriate cortex of behaving rhesus monkey. *J Neurophysiol* 40:1392–1405.
32. Freeman RD, Ohzawa I (1990) On the neurophysiological organization of binocular vision. *Vision Res* 30:1661–1676.
33. Parker AJ, Smith JE, Krug K (2016) Neural architectures for stereo vision. *Philos Trans R Soc Lond B Biol Sci* 371:20150261.
34. Chen G, Lu HD, Tanigawa H, Roe AW (2017) Solving visual correspondence between the two eyes via domain-based population encoding in nonhuman primates. *Proc Natl Acad Sci USA* 114:13024–13029.
35. Xu H, et al. (2016) Rivalry-like neural activity in primary visual cortex in anesthetized monkeys. *J Neurosci* 36:3231–3242.
36. Hallum LE, et al. (2017) Altered balance of receptive field excitation and suppression in visual cortex of amblyopic macaque monkeys. *J Neurosci* 37:8216–8226.
37. Jazayeri M, Lindbloom-Brown Z, Horwitz GD (2012) Saccadic eye movements evoked by optogenetic activation of primate V1. *Nat Neurosci* 15:1368–1370.
38. Gerits A, et al. (2012) Optogenetically induced behavioral and functional network changes in primates. *Curr Biol* 22:1722–1726.
39. Ohayon S, Grimaldi P, Schweers N, Tsao DY (2013) Saccade modulation by optical and electrical stimulation in the macaque frontal eye field. *J Neurosci* 33:16684–16697.
40. Dai J, Brooks DI, Sheinberg DL (2014) Optogenetic and electrical microstimulation systematically bias visuospatial choice in primates. *Curr Biol* 24:63–69.
41. May T, et al. (2014) Detection of optogenetic stimulation in somatosensory cortex by non-human primates—Towards artificial tactile sensation. *PLoS One* 9:e114529.
42. Marik SA, Yamahachi H, Meyer zum Alten Borgloh S, Gilbert CD (2014) Large-scale axonal reorganization of inhibitory neurons following retinal lesions. *J Neurosci* 34:1625–1632.
43. Acker L, Pino EN, Boyden ES, Desimone R (2016) FEF inactivation with improved optogenetic methods. *Proc Natl Acad Sci USA* 113:E7297–E7306.
44. MacDougall M, et al. (2016) Optogenetic manipulation of neural circuits in awake marmosets. *J Neurophysiol* 116:1286–1294.
45. Ranck JB, Jr (1975) Which elements are excited in electrical stimulation of mammalian central nervous system: A review. *Brain Res* 98:417–440.
46. Yizhar O, Fenno LE, Davidson TJ, Mogri M, Deisseroth K (2011) Optogenetics in neural systems. *Neuron* 71:9–34.
47. Lu HD, Chen G, Tanigawa H, Roe AW (2010) A motion direction map in macaque V2. *Neuron* 68:1002–1013.
48. Santhanam G, Sahani M, Ryu S, Shenoy K (2004) An extensible infrastructure for fully automated spike sorting during online experiments. *Conf Proc IEEE Eng Med Biol Soc* 6:4380–4384.
49. Shin Y, Kwon HS (2016) Mesh-based Monte Carlo method for fibre-optic optogenetic neural stimulation with direct photon flux recording strategy. *Phys Med Biol* 61:2265–2282.